

DIFFUSIONAL REACTION RATES THROUGH THE Nb WRAP IN SSC AND OTHER ADVANCED MULTIFILAMENTARY Nb 46.5WT %Ti COMPOSITES

+K. J. Faase, +P. J. Lee, *J. C. McKinnell, +D. C. Larbalestier
+University of Wisconsin-Madison, Applied Superconductivity Center, Madison, WI
*Superconductor Development Division, TWCA, Albany, OR 97321

ABSTRACT

Diffusional reaction rates through the Nb barrier of Superconducting Super Collider (SSC) Phase I & II research and development conductors have been measured. A Nb foil wrap is used as a diffusion barrier around the Nb-Ti filaments in order to minimize the reaction between the Ti and the surrounding Cu matrix. SSC wires with a range of barrier thicknesses (~ 0.1 - $5 \mu\text{m}$), were heat treated at elevated temperatures (530 - $700 \text{ }^\circ\text{C}$) at their final heat treatment size. Compositional analyses were performed by electron microprobe, and scanning Auger microscopy. Starting from the Cu matrix, we found a solid solution of Ti deep into the Cu, followed by a layer of TiCu_4 immediately outside the Nb wrap, which contained substantial Cu and Ti. Underneath the wrap was a fine-scale mixture of unidentified intermetallics and solid solution containing all 3 elements. The parabolic growth rates of these reaction layers were measured and the fastest reaction was found to be the diffusion of Cu, first through the Nb and then through the Nb-Ti under the barrier. Thus the major reaction occurs *under* the barrier. The growth rates followed an Arrhenius behavior with temperature. Extrapolation of the results to lower temperatures predicts that a uniform 1.5 vol % Nb barrier would protect a $6 \mu\text{m}$ filament for 40 hrs. at $375 \text{ }^\circ\text{C}$ but that a 4 % barrier would be needed to protect the same filament for 80 hrs. at $420 \text{ }^\circ\text{C}$. Present SSC production experience is in good agreement with these predictions.

INTRODUCTION

It is well documented that the critical current density, J_c , of Nb 46.5w %Ti superconducting wire composites is enhanced by an optimized heat treatment and wire drawing process.^{1,2,3} Heat treatments at about $400 \text{ }^\circ\text{C}$ nucleate α -Ti precipitates in the grain boundaries of the Nb-Ti β -phase matrix. These α -Ti precipitates are then reduced to nanometer-scale ribbons upon final wire drawing. These α -Ti ribbons are the prime flux pinning centers in Nb-Ti and their density and size thus control the intrinsic J_c . J_c is strongly dependent on the volume % α -Ti, which is enhanced by longer, more frequent heat treatments.^{2,4} Unfortunately, aggressive high temperature heat treatments tend to introduce an extrinsic limit on the transport critical current density, J_{ct} , thus reducing J_{ct} below J_c . The principal reason is that brittle intermetallic compounds tend to form at the matrix-filament interface during heat treatments and these do not deform well during wire drawing, thus resulting in filament sausaging.^{6,7}

The most widely used method of controlling this problem is to surround the filament with a Nb diffusion barrier.^{8,9} Unfortunately neither Nb, nor any other practical choice, is totally impermeable to Cu and Ti. To maximize the J_c performance of a given composite, the Nb wrap thickness must be thick enough to minimize intermetallic formation but not be so thick that too much superconductor volume is occupied by Nb. This optimization problem stimulated the present work. The goal was to understand intermetallic reaction rates through the Nb barrier so that the effect of changing various processing parameters such as the Nb wrap thickness, the heat treatment duration and temperature could be rationally assessed. A companion paper by High et al.¹⁰ describes the consequences of these reactions for filament sausaging and their influence on the transport critical current densities of similar composites.

Table 1. Composite details

Composite sample identity	R+D Phase	as received condition of composite	Size at which composite was heat treated	Nb:NbTi area cross-section ratio	Average Nb thickness at HT size	Design filament diameter at 0.318" wire diameter
OST1836-1*	I	1.03" diameter multifilamentary billet	0.365"	1 %	0.2 ± 0.1 μm	6 μm
SC2096-1*	I	0.862" diameter multifilamentary billet	0.365"	2 %	0.35±0.15 μm	9 μm
IGC5263-3**		1.03" diameter multifilamentary billet	0.325"	2 %	1.2±0.3 μm	20 μm
SC2444-2	II	1.03" diameter multifilamentary billet	0.325"	4 %	0.4±0.15 μm	6 μm
OST2164	II	0.120" monofilament wire	0.144"	4 %	3.7±0.9 μm	

* the 192 hr/680 °C samples were heat treated at 0325".

** IGC5263-3 is a Fermilab Quadrupole composite.

EXPERIMENTAL DETAILS

The diffusional reaction zones produced by standard processing heat treatments (3-160 hr/300-420 °C) are at a sub-micron scale and are very difficult to analyze quantitatively even when no diffusion barrier is present.⁷ Thus, to aid microscopic examination of the reaction zones, heat treatments were exaggerated by performing them in the range of 10-192 hr at 530-700 °C. These exaggerated heat treatments allowed the extent of the reaction zones and their composition to be examined better by Scanning Electron Microscopy in Back Scatter mode (SEMBS), Electron Microprobe Analysis (EPMA) and by the Scanning Auger Microprobe (SAM).

The materials chosen for this study were 6 μm and 9 μm filament diameter composites produced under the SSC phase I & II research and development exercises. An additional composite fabricated for a recent low β quadrupole beam line at Fermilab was also examined.¹¹ This composite had a 20 μm filament diameter at the SSC inner conductor final wire size and its Nb diffusion barrier was both thicker and more uniform than was the case for the SSC composites. The materials were all received after composite billet extrusion at about 1" diameter and were subsequently drawn and processed in our laboratory. Samples were heat treated in vacuum (<10⁻⁴ torr) furnaces under conditions listed in Table 1 and Table 2.

The heat treated samples were mounted in conductive Bakelite and mechanically ground and polished. A JEOL35C SEM was used in back scatter mode in order to provide micrographs with good atomic number contrast. Compositions, calibrated against elemental standards, were measured on an ARL EMX 30 microprobe to a spatial resolution of 1-2 μm. Higher spatial resolution scans (0.1-0.2 μm) were performed on a Phi660 SAM. However, these scans are only semi-quantitative.

Table 2. Parabolic reaction rate constants D_Y [m²/sec], and Arrhenius reaction constants.

Designation	Reaction	Parabolic reaction rate constants [m ² /sec]					D_0 [m ² /sec]	Q [kJ/mole]
		700 °C	680 °C	630 °C	580 °C	530 °C		
NbCu	Cu through Nb	7.5*10 ⁻¹⁶	4.8*10 ⁻¹⁶		7.4*10 ⁻¹⁷		7.5*10 ⁻⁹	130
Cu	Cu into NbTi		8.9*10 ⁻¹⁷	3.0*10 ⁻¹⁷	8.1*10 ⁻¹⁸	1.4*10 ⁻¹⁸	1.5*10 ⁻⁷	161
NbTi	Ti through Nb wrap		7.7*10 ⁻¹⁶	2.6*10 ⁻¹⁶	2.7*10 ⁻¹⁷		0.0024	228
Ti	Ti into Cu		1.6*10 ⁻¹⁸	7.7*10 ⁻²⁰	1.4*10 ⁻²⁰		0.019	301

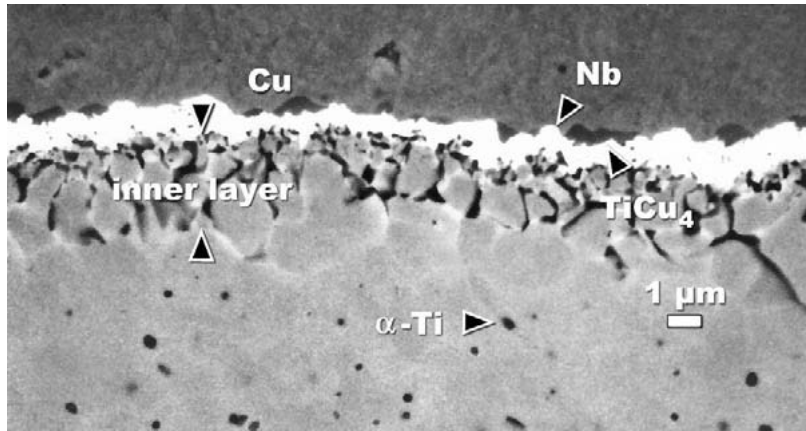


Figure 1. SEMBS micrograph of IGC5263-3 reacted for 192 hr/580 °C.

An example of the reacted layer observed after an intermediate amount of reaction is shown in Figure 1. In general, the reaction layer found outside the Nb barrier and the barrier itself were both well-defined in thickness. However, the reaction layer underneath the barrier was complex and gave much evidence of intergranular phases, as well as a substantial solid solution layer. The scale of this was generally too small to measure quantitatively with the EPMA. In order to better define the thickness of the inner layer, a boundary was marked onto a transparent overlay of the SEMBS image. Layer thicknesses were then measured from these SEMBS micrographs using a high resolution (1024 x 1024) Image Analysis (IA) system. The initially high contrast level of the SEMBS images was further enhanced by making a binary image with the IA. The IA system then placed a matrix of ~300 closely-spaced, parallel straight lines perpendicular to the reaction interfaces onto the image. The intercepts of these lines with the interfaces were digitally computed by the IA system and the average and standard deviations of these reaction layers were recorded.

RESULTS

A compositional gradient measured by EPMA on a SC2096-1 sample reacted for 192 hr at 680 °C is shown in figure 2. Traces of Ti are found in the Cu matrix to a depth of ~20μm outside the Nb diffusion barrier. This is consistent with the equilibrium solubility of Cu in Ti, which is reported to be ~3at. % at 680 °C.¹² Immediately on the outside of the barrier is a layer of well-defined composition, TiCu₄. This layer is somewhat irregular in thickness, however. Next comes the barrier layer, which now contains Ti and Cu. Since the Nb started out only being 0.35 μm thick at the heat treatment size, its composition cannot be accurately identified by EPMA. The matrix immediately under the barrier was heavily reacted, consisting of a mixed layer of intermetallics and solid solution of Cu, Nb and Ti forming a layer 20-25μm thick. Beyond this layer, traces of Cu are seen more than 30μm into the filament. Accurate quantification of these inner layers could not be made because the features are on a scale too fine for the EPMA.

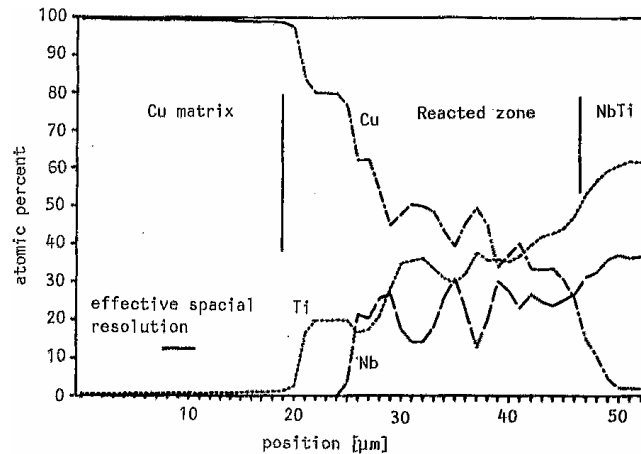


Figure 2. Electron microprobe composition profile across the Cu-Nb-NbTi interface region of one filament of SC2096-1 reacted for 192 hr/680 °C.

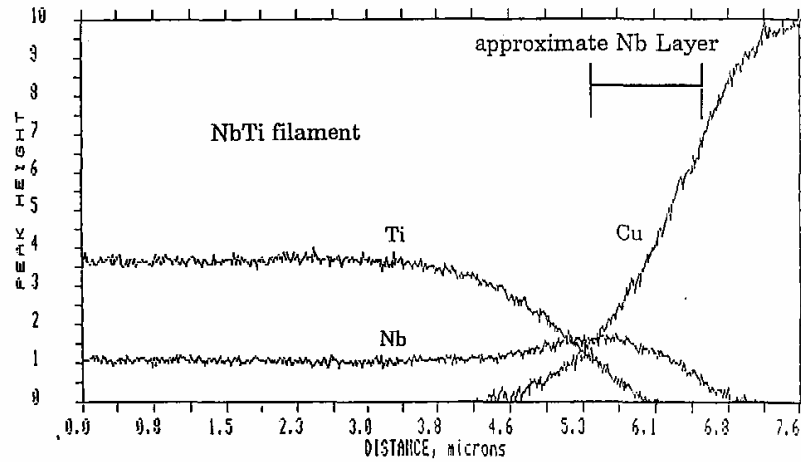


Figure 3. SAM compositional profile of across the Nb wrap of a filament of IGC5263-3 at 0.325" reacted for 160 hr/420 °C.

A SAM compositional profile, figure 3, was performed on the same composite heat treated at a lower temperature (160 hr/420 °C). No metallographic evidence of reaction was observed in the SEMBS micrograph. However, the SAM profile shows that Cu has diffused through the Nb wrap and into the Nb-Ti filament but Ti has only diffused approximately half way through the Nb wrap at this stage. Thus it appears that the most rapid step is the diffusion of Cu through the Nb barrier, even though the published phase diagrams report that Cu and Nb have only a very small mutual solubility.¹³

An SEMBS micrograph of the thicker barrier, larger filament IGC5263-3 composite reacted less aggressively for 192 hrs at 580 °C is shown in figure 1. Outside the white Nb barrier (~1 μm thick) is an irregular layer (<1 μm thick) of TiCu₄. Inside the Nb wrap is a ~2-4 μm thick layer of mixed Nb, Ti and Cu intermetallics and solid solution. Heavy infiltration along the Nb-Ti grain boundaries has occurred. α-Ti precipitates appear black in SEMBS mode and can be seen 5-10 μm into the filament. However, they appear to be absent in the reaction zone immediately under the barrier.

Detailed image analysis of the reaction zones was performed on sixteen reacted IGC5263-3 samples. This composite was chosen because it had the thickest and most uniform barrier. The SEMBS images were analyzed by dividing the reaction zones into three distinct layers. The outer zone was the well-defined TiCu₄ layer, the second layer was the Nb wrap, and the inner layer was the reaction layer underneath the barrier. Layer thicknesses are plotted against the square root of time in figures 4a-d. The thickness data follow a square root time dependence quite well, as would be expected for diffusion at a planar, infinite sink interface. The inner and outer layer thicknesses were fit to the following expression:

$$X=[D_Y(t-t_0)]^{1/2}$$

where x = layer thickness[μm], $D_Y=D_{Cu \text{ (or Ti)}}$ is the parabolic reaction rate constant [m²/sec] of Cu (or Ti) diffusing into the NbTi filament (or Cu matrix), t_0 [hr] is the time it takes Cu (or Ti) to diffuse through the Nb layer, and t [hr] is the time that the Cu (or Ti) has to diffuse into the NbTi filament (or Cu matrix). The reaction rate constant for diffusion through the Nb wrap is then described by:

$$D_Y=x^2 \text{ barrier} / t_0$$

where X_{barrier} = barrier thickness [m], $D_Y = D_{NbCu \text{ (or NbTi)}}$ is the parabolic reaction rate constant of Cu (or Ti) diffusing through the Nb wrap [μm²/ hr], and t_0 is time it takes for Cu (or Ti) to diffuse through the Nb layer[hr].

The reaction rate constants from Table 2 were plotted against inverse absolute temperature in an Arrhenius plot (figure 5). All four parabolic reaction rate constants fit the Arrhenius expression:

$$D_Y(T) = D_{0Y}e^{(-Q/RT)}$$

where $D_Y(T)$ is the parabolic reaction rate constant [m²/sec] at temperature, T[K], D_{0Y} is the Arrhenius prefactor [m²/sec], Q is the activation energy [J/mole], and R is the gas constant [$R = 8.314 \text{ J/(Kmole)}$].

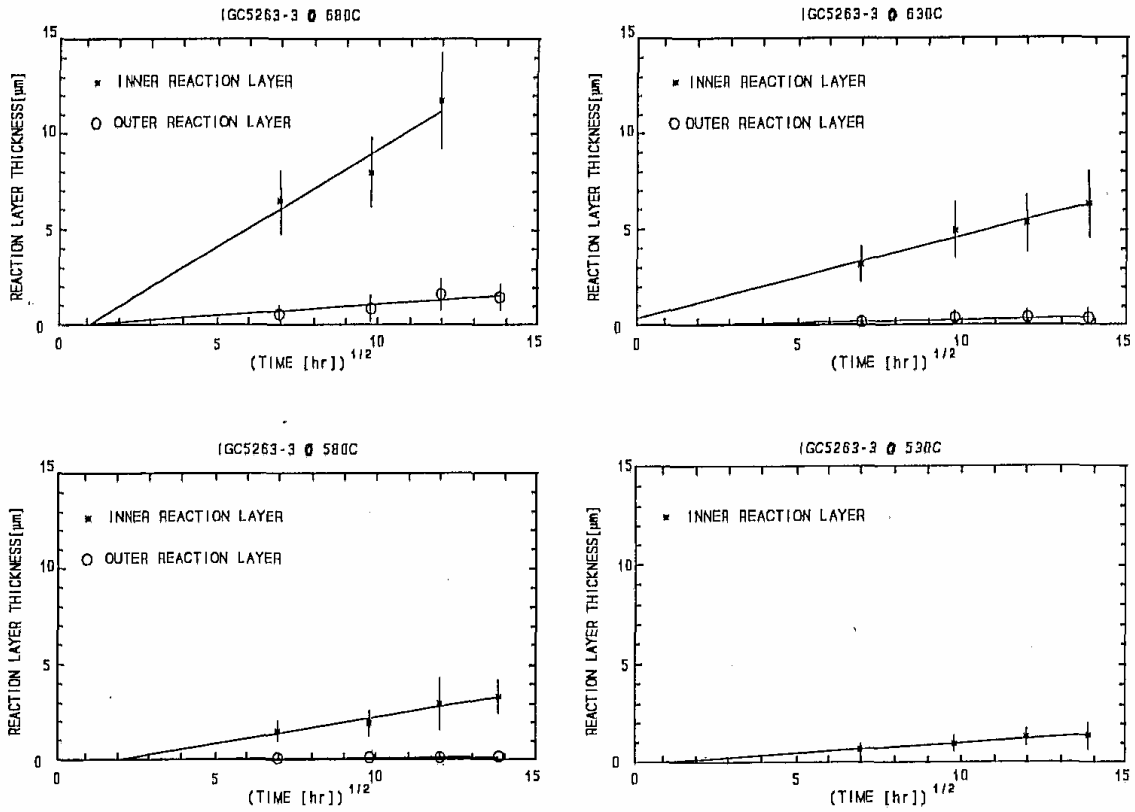


Figure 4. Inner and outer reaction layer thicknesses [μm] plotted against square root of time [hr].

DISCUSSION

Although the diffusion reactions occurring during the heat treatment are complex and we have not been able to identify all of the phases which occur, the present results do form a consistent whole. The reaction rate data fit the expected parabolic form well and the temperature dependence of the reaction rates is also well behaved. The activation energies for the reactions fall into the reasonable range of 130 to 301 kJ/mole. This range is a little larger than that found in the earlier study on unclad filaments⁷, where values of 117 and 205 kJ/mole were obtained for the inner and outer reaction layers, respectively. In this case the inner and outer layers had values of 161 and 301 kJ/mole. This variation suggests that diffusion is defect-controlled, a result to be expected by the low temperature of the reactions (600 °C is ~ 0.4 and $\sim 0.3 T_m$ for Nb-Ti and Nb, respectively). The intergranular penetration of Cu in the Nb-Ti filament is direct evidence of grain boundary diffusion and this is consistent with the result that the lowest energy reaction (130 kJ/mole) is

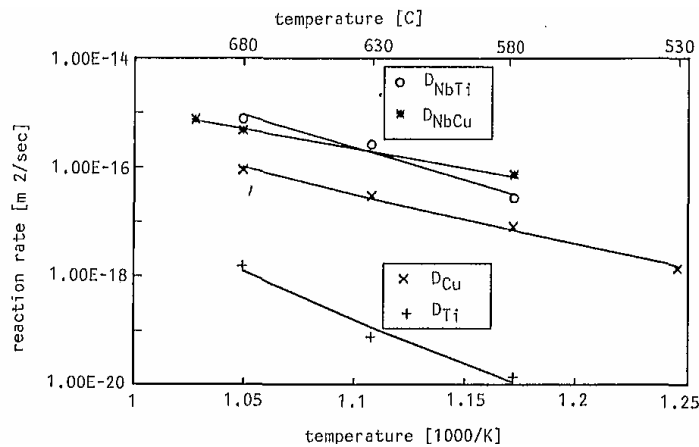


Figure 5. Arrhenius plot of D_Y [m^2/sec] against inverse, absolute temperature [$1/\text{K}$]. See Table 2 for nomenclature.

for the diffusion of Cu through the Nb barrier. This latter result was unexpected, in that Cu and Nb have little mutual solubility.¹³ Diffusion of Cu along the Nb grain boundaries is the most reasonable mechanism by which Cu can pass so rapidly through the Nb. Although the present results confirm that Nb barriers are not impervious to Cu and Ti, they do greatly inhibit the reaction. Reaction rates were between one and two orders of magnitude lower in the Nb-wrapped barrier, as compared to the unclad filaments.⁷

One major difference between the diffusion reactions, with and without the Nb barrier, concerns perceptions of how the breakdown of the barrier can best be observed. The normal diagnostic is to examine exposed filaments by SEM for any sign of intermetallic nodule formation. The present results show that the fastest reaction occurs *under* the barrier. Thus, the reaction is not necessarily visible from the outside, unless the drawing process has caused the layer and its surrounding Nb layer to fracture. Thus, examination late in the drawing process will be necessary to check this point.

The data were all taken at temperatures between 530 and 680 °C, in order to make the reaction layers large enough to study, much as we did in the earlier study of Larbalestier, Lee and Samuel on unclad filaments.⁷ With the exception of the points noted above, the present results are generally consistent with this earlier study and with the studies of Garber et al.¹⁴ and Taillard et al.¹⁵ One particular point is that the Ti-rich phase has the composition TiCu_4 , as earlier reported in ref. 14, rather than the Ti_2Cu_7 composition that we saw earlier.⁷

One of the key tests of the utility of this data is in the prediction of what Nb barrier thicknesses are needed to protect fine filament conductors during processing. We here consider the application to SSC style conductors having filament sizes of 2.5 and 6 μm . Processing choices for such conductors lie between two poles: on one side the temperature and time of heat treatments are restricted so as to minimize barrier damage, while on the other the maximum amount of flux pinning is developed by extending the heat treatments. Until now, most barriers have been too thin or variable to support the second strategy. Representative heat treatments which describe the two cases are 3 H.T. of 40 hrs at 375 °C and 3 of 80 hrs at 420 °C. As is well-documented², the latter treatment produces a higher intrinsic J_c . However, any advantage of the more extended heat treatments is easily lost by sausing of SSC 6 μm dia. filaments when only a 2 % Nb barrier (expressed as a percentage of the total filament area) is used, as is described in detail in the companion paper by High et al.¹⁰ Thus, control of the filament sausing has been the central thrust of SSC conductor R+D, a point further reinforced by the role that sausing plays in reducing piece length, increasing the low field magnetization and generally contributing to unpredictable and non-uniform properties.

Although extrusion temperatures lie in the general range studied, pre-heat times, being generally of the order of an hour, are much shorter than were studied here. Table 3 considers various cases of interest for 2.5, 6 and 9 μm filament conductors. Since the fastest event is always the diffusion of Cu through the Nb barrier, whatever the temperature, we have taken this as the first criterion of damage to the barrier. Table 3 shows that even a 2 % barrier on a 2.5 μm filament conductor requires 88 hrs. at 650 °C before the Cu has penetrated through to the Nb-Ti. Thus breakdown at extrusion size is never likely to be a problem. This reinforces our earlier conclusions for bare filament conductors that the problem comes during the J_c optimization heat treatments, especially the final heat treatment.⁷

Table 3 computes various options for the barrier thickness and percentage corresponding to such a final heat treatment. In the first SSC R+D Phase, 1-2 % barriers were used, this increasing to 4 % for Phase II. In principle, a 2 % barrier on a 6 μm filament would protect for 107 hrs at 375° C. However, a treatment of 80 hrs. at 420 °C would require at least a 4 % barrier. The intrinsic J_c of the second H.T. is at least 10 % higher, thus giving a net benefit. The same benefit can be obtained by extending the number or time of the 375 °C H.T. These predictions are in excellent agreement with the J_c and filament sausing results obtained by High et al.¹⁰ on these same composites. The results of Table, 3 are also of interest for the development of 2.5 μm filament conductors. The table predicts that full benefit would be require a 9 % Nb barrier.

Figure 6 is a schematic of conventionally heat treated SSC transverse cross sections depicting the microstructural difference between unreacted and diffusionally reacted samples. Figure 6a is the ideal case of a continuous Nb wrap, thick enough to hinder any diffusional reactions in the wire composite. The microstructure of the filament shows large α -Ti precipitates growing in close proximity to the Nb wrap and is free of the TiCu_4 layer outside of the Nb wrap. On the other hand, figure 6b exhibits the microstructural consequences of a thin, irregular Nb wrap. The microstructure directly under the barrier is then altered by the diffusion of Cu through the inadequate Nb barrier. The presence of the diffused Cu has apparently restrained the growth of the α -Ti precipitates. Moreover, a submicron layer of TiCu_4 has formed at the Nb wrap puncture.

Table 3. Calculations of t_0 , and reaction zone lengths

time [hr]	tem p. [C]	wire comp. dia [in]	barrier thick, [μm]	AREA % Nb-NbTi			t_0 -Cu [hr]	t_0 -Ti [hr]	x_{inner} [μm]	X_{TiCu_4} [μm]
				2.5 μm	6 μm filame	9 μm filament				
1	550	12	10	4.2	1.8	1.2	695	3270	0	0
3	550	12	10	4.2	1.8	1.2	695	3270	0	0
1	650	12	10	4.2	1.8	1.2	88	89	0	0
3	650	12	10	4.2	1.8	1.2	88	89	0	0
40	375	0.325	0,0	0.0	0.0	0.0	0	0	0.048	0*
40	375	0.325	0.2	3.1	1.3	0.9	47	10500	0	0
40	375	0.325	0.3	4.7	2.0	1.3	107	23600	0	0
40	375	0.325	0.4	6.3	2.6	1.7	191	42000	0	0
40	375	0,325	0.5	7.8	3.3	2.2	298	65600	0	0
80	420	0.325	0.0	0.0	0.0	0.0	0	0	0.18	$3.4 \cdot 10^{-4}$
80	420	0.325	0.2	3.1	1.3	0.9	10	674	0.17	0
80	420	0.325	0.4	6.3	2.6	1.7	40	2700	0.13	0
80	420	0.325	0.6	9.4	3.9	2.6	89	6070	0	0
80	420	0.325	0.8	12.5	5.2	3.5	159	10800	0	0

*unrealistic sub-angstrom value.

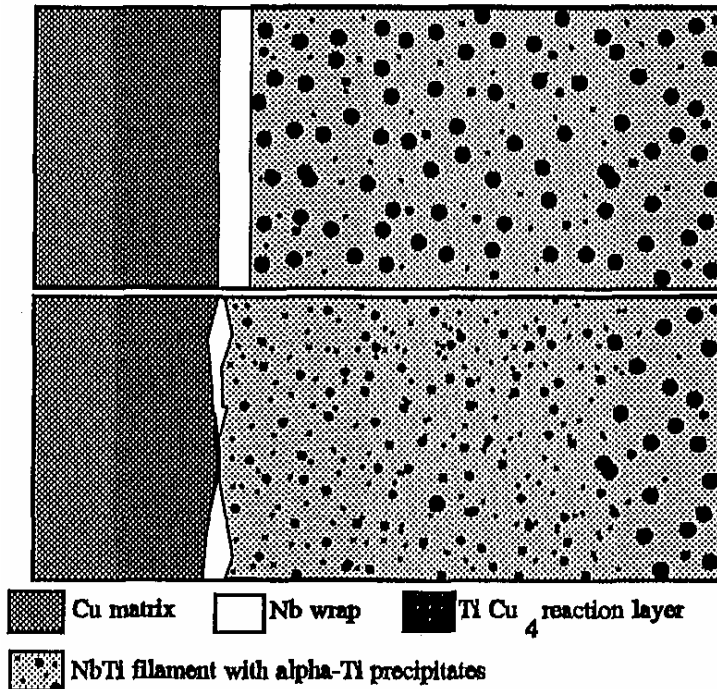


Figure 6. Schematic transverse section a.) an ideal Nb layer and of b.) an inadequate, discontinuous layer with its resultant "Cu-poisoned" layer and the outer reaction layer.

Although the volume percent of α -Ti precipitates in the diffusionally reacted perimeter of the OST1836-1 filaments have not been quantified, it is likely that the interdiffused Cu is deleterious to the overall performance of the composite. Comparisons between transverse and longitudinal cross sections of SSC filaments show that filaments containing the "Cu poisoned-zone" have been compromised by sausageing upon ensuing wire drawing, while diffusionally unreacted samples are free of filament sausageing. Furthermore, Moreland et. al.¹⁶ found that Cu concentrations of < 3 % in the perimeter of the NbTi filaments degrade the local energy gap. Thus the interdiffusion reactions occurring under the Nb barrier are complex and may need careful attention as the SSC conductor goes into full-scale production. We finally note that the present work here has only considered the grossest scale effects of the diffusion process. The interdiffused Cu which penetrates the barrier may also degrade filament quality for the extreme strain conditions under which Nb-Ti composites reach their peak J_c .

CONCLUSIONS

1. The most rapid action is for the diffusion of Cu through the Nb wrap. Diffusion into the Nb-Ti filament beneath the barrier is also very rapid. This reaction *under* the barrier is more rapid than that which occurs outside the barrier.
2. The reaction rates closely fit an Arrhenius equation, allowing calculation of an optimal Nb diffusion barrier thickness in SSC wire composites. These calculations indicated that a Nb wrap thickness of 0.6 μm would prevent the diffusion of Cu into the NbTi filament during an 80 hr/420 °C heat treatment. For typical SSC composites this represents barrier proportions of ~2.5 % and ~4 % respectively for 9 and 6 μm filament wires and 9 % for 2.5 μm filament wires.

Acknowledgements-We would like to thank William Starch, Yvonne High, Everett Glover, Rick Noll and Ngoc Tran for their experimental assistance. The composites were supplied through collaborations with R. M. Scanlan (LBL), D. Capone (SSCL), and A. D. McInturff (FNAL) with composites produced Intermagnetics General Corp., Oxford Superconducting Technology, and Supercon. The work was supported by the SSC Laboratory and the DOE-Office of High Energy Physics, GRANT# DE-AC02-82ER-4007

References

- 1 P. J. Lee and D. C. Larbalestier, Acta. Metall. 35:2523 (1987).
- 2 L. Chengren and D. C. Larbalestier, Cryogenics 27:171 (1987).
- 3 C. Meingast and D. C. Larbalestier, J. Appl. Phys. 66:5960 (1989).
- 4 P. J. Lee, J. C. McKinnell and D. C. Larbalestier, Adv. Cryo. Eng. 36:287 (1990).
- 5 P. J. Lee, and D. C. Larbalestier, J. Mat. Sci. 23:3951 (1988).
- 6 H. Hillman, Superconductor Materials Science. Plenum Press, p. 275., 1981.
- 7 D. C. Larbalestier, P. J. Lee and R. W. Samuels, Adv. Cryo. Eng. 32:716 (1986).
- 8 R. Scanlan and T. Kirk, SSC-MAG-M4141 (1988).
- 9 R. M. Scanlan, J. Royet, and R. Hannaford, IEEE Trans. Mag. 23:1719 (1987).
- 10 Y. E. High, P. J. Lee, J. C. McKinnell and D. C. Larbalestier. Submitted to ICMC 1991.
- 11 R. W. Hanft, B. C. Brown, D. A. Lamm, A. D. McInturff, and M. J. Syphers, IEEE Trans. Mag. 25:1647 (1990).
- 12 M. Hansen. Constitution of Binary Alloys. McGraw-Hill, p. 643., 1958.
- 13 H. P. Elliot. Constitution of Binary Alloys. First Supplement McGraw-Hill, p. 253., 1965.
- 14 M. Garber, M. Suenaga, W. B. Sampson, R. L. Sabatini, IEEE Trans. NS. 32:3681 (1985).
- 15 R. Taillard, C. E. Bruzek, J. Foct, H. G. Ky, A. Lacaze and T. Verhaege, Adv. Cryo. Eng. 36:303 (1989).
- 16 J. Moreland, J. W. Ekin and L. F. Goodrich, IEEE Trans. Mag. 23:1101 (1985).